European Society for Paediatric Research
Society for Pediatric Research
www.nature.com/pr

BASIC SCIENCE ARTICLE

Butyrate induces development-dependent necrotizing enterocolitis-like intestinal epithelial injury via necroptosis

Kewei Wang[1,2], Guo-Zhong Tao[1]✉, Fereshteh Salimi-Jazi[1], Po-Yu Lin[1], Zhen Sun[1], Bo Liu[1], Tiffany Sinclair[1], Mirko Mostaghimi[1], James Dunn[1] and Karl G. Sylvester[1,3]✉

BACKGROUND: The accumulation of short-chain fatty acids (SCFAs) from bacterial fermentation may adversely affect the underdeveloped gut as observed in premature newborns at risk for necrotizing enterocolitis (NEC). This study explores the mechanism by which specific SCFA fermentation products may injure the premature newborn intestine mucosa leading to NEC-like intestinal cell injury.
METHODS: Intraluminal injections of sodium butyrate were administered to 14- and 28-day-old mice, whose small intestine and stool were harvested for analysis. Human intestinal epithelial stem cells (hIESCs) and differentiated enterocytes from preterm and term infants were treated with sodium butyrate at varying concentrations. Necrosulfonamide (NSA) and necrostatin-1 (Nec-1) were used to determine the protective effects of necroptosis inhibitors on butyrate-induced cell injury.
RESULTS: The more severe intestinal epithelial injury was observed in younger mice upon exposure to butyrate ($p = 0.02$). Enterocytes from preterm newborns demonstrated a significant increase in sensitivity to butyrate-induced cell injury compared to term newborn enterocytes ($p = 0.068$, hIESCs; $p = 0.038$, differentiated cells). NSA and Nec-1 significantly inhibited the cell death induced by butyrate.
CONCLUSIONS: Butyrate induces developmental stage-dependent intestinal injury that resembles NEC. A primary mechanism of cell injury in NEC is necroptosis. Necroptosis inhibition may represent a potential preventive or therapeutic strategy for NEC.

Pediatric Research (2023) 93:801–809; https://doi.org/10.1038/s41390-022-02333-z

IMPACT:

- Butyrate induces developmental stage-dependent intestinal injury that resembles NEC.
- A primary mechanism of cell injury caused by butyrate in NEC is necroptosis.
- Necroptosis inhibitors proved effective at significantly ameliorating the enteral toxicity of butyrate and thereby suggest a novel mechanism and approach to the prevention and treatment of NEC in premature newborns.

INTRODUCTION

Necrotizing enterocolitis (NEC) has been intensely studied for decades, yet its precise etiology remains elusive and associated morbidity and mortality high.[1,2] Infection, incomplete or diminished intestinal barrier function, and suboptimal innate immune response along with altered intestinal microbiota have all been implicated as leading explanatory variables making significant contributions to the pathophysiology of NEC.[2–6] Although various measures have shown some promise in reducing NEC occurrence, its incidence remains highly variable between and within neonatal intensive care units.

The mammalian newborn gut undergoes rapid postnatal adaptation to enteral nutrition that includes colonization and establishment of the intestinal microbiota. The interaction between colonizing bacteria and the newborn host results in metabolites that act as important mediators for metabolism and immunity. The premature newborn gut is marked by reduced peristalsis, decreased tight junctions, and decreased epithelial mucus production along with immature brush-border enzymes leading to malabsorption.[7,8] Together, these changes may render the premature gut prone to injuries by bacterial metabolites that are ordinarily present and are not harmful in the term infant gut.[9,10] Short-chain fatty acids (SCFAs) are particularly abundant by-products of bacterial fermentation of enteral carbohydrates and lipids. Abnormal accumulation of SCFAs specifically butyrate has been previously observed in the intestinal lumen of human infants with NEC.[11] The intestinal lumen maintains a butyrate gradient from the villus tip to the crypt as fully differentiated enterocytes metabolize butyrate whereas the same relative concentration is toxic to stem cells and progenitor cells.[12] High concentrations of butyrate have been demonstrated to cause intestinal necrosis similar to NEC in animal models.[13,14]

[1]Department of Surgery, Stanford University School of Medicine, Stanford, CA, USA. [2]Department of Gastrointestinal Surgery, The First Hospital of China Medical University, 110001 Shenyang, Liaoning Province, China. [3]Stanford Metabolic Health Center, Stanford University School of Medicine and Stanford Healthcare, Stanford, CA, USA.
✉email: gtao@stanford.edu; Sylvester@stanford.edu

Received: 25 March 2022 Revised: 12 September 2022 Accepted: 18 September 2022
Published online: 6 October 2022

Preterm NEC occurs exclusively in newborns born prematurely at less than 32 weeks completed gestational age and of very low (<1500 g) (VLBWs) or extremely low (<1000 g) birth weight (ELBWs). In these defined at-risk populations, we posit that the gastrointestinal mucosa is particularly vulnerable to the primary by-products that accumulate as a result of enteric microbial colonization and fermentation. The combination of gut colonization and the introduction of enteral feedings are nearly ever-present in classically described preterm NEC. Thus, we reasoned that specific SCFA would produce an injury pattern of the mucosa that varies by stage of development. In the current study, we aimed to explore the effect of butyrate on intestinal epithelial cells at varying degrees of development and differentiation.

MATERIALS AND METHODS

Reagents

K18 Asp237 (AnaSpec, Fremont, CA), anti-keratin 8 antibodies (Troma-1, MilliporeSigma, Temecula, CA), pMLKL (Abcam, Cambridge, MA), PGC-1α, caspase 3, cleaved caspase 3, and anti-GAPDH (Cell Signalling Technology Inc., Danvers, MA), Alexa Fluor® 488 Goat Anti-Rat (IgG) secondary antibodies (Abcam, Cambridge, MA), necrosulfonamide (NSA) (Selleck Chemical LLC, Houston, TX), and necrostatin-1 (Nec-1) (Santa Cruz Biotechnology Inc., Dallas, TX) were used. All other chemicals were purchased from Sigma.

Mouse model

All animal experiments were conducted under a protocol approved by the Stanford University School of Medicine Institutional Animal Care and NIH guidelines. FVB/N mice aged 14 days (P14) or 28 days (P28) were chosen for a determination of in vivo injury. The abdomen was entered via midline laparotomy with a 1.5 cm incision. After exposure of the ileocecal junction, a sterile solution of sodium butyrate (NaBu) at a concentration of 150 mM (pH 7.2) or phosphate buffered saline (1× PBS, pH 7.4) as a salt control with similar adjusted pH and osmolarities was injected directly into the intestinal lumen with a volume of 10 µL per gram of body weight using a 27-gauge needle with the flow directed toward the proximal small intestine. The abdominal wall was then closed in two layers using 4-0 Vicryl sutures. After 24 h, the mice were sacrificed, and their stools and small intestines were harvested and stored either at −80 °C or formalin-fixed. An equal amount (in weight) of stool samples was mixed with 1× Laemmli sample buffer (0.1 g stool per mL), followed by homogenization, heat-denaturing, and centrifugation, then 10 µL of the subsequent supernatants were loaded to each lane of the gel for comparison.

Histology

Intestinal tissues were fixed in 10% PBS-buffered formalin, embedded in paraffin and 5-µm-thick sections were stained with hematoxylin–eosin (H&E) (ScyTek Laboratories, Inc., Logan, UT) according to standard protocol. Samples were evaluated by two blinded pathologists. The presence of NEC was confirmed using published tissue injury criteria for necrotic lesions and NEC severity was graded on a 5-point scale according to the published data on NEC mouse models with grade 0: no injury, grade 1: mild separation of lamina propria, grade 2: moderate separation of the submucosa, grade 3: severe separation and/or edema in the submucosa and grade 4: transmural necrosis.[15,16]

Immunofluorescence (IF) staining

IF staining was performed to demonstrate the localization and abundance of keratin 8 (K8) in the intestine. Mouse intestines were fixed with acetone and incubated initially with anti-K8 antibodies (Troma-1, MilliporeSigma, Temecula, CA, 1:50) and subsequently with 4 µg/mL Alexa Fluor® 488 Goat Anti-Rat (IgG) secondary antibodies (Abcam, Cambridge, MA). The slides were counterstained with DAPI (Cell Signalling Technology (CST), Danvers, MA) and observed under a Zeiss LSM 510 confocal microscope (Carl Zeiss, Jena, Germany).

HT29 cells were double-stained with Hoechst 33342 and propidium iodide (PI) (Genscript, Piscataway, NJ) after butyrate treatment to detect cell death. The treated cells were then viewed under fluorescent microscopy.

Human intestinal cell culture and injury model

The procurement of newborn intestine for culture was approved by the institutional review board of Stanford University. Written informed consent was obtained for intestine sampling from both parents of all neonates who had bowel resection for surgical issues other than NEC. The gestational age of the preterm infant was 25 weeks. Day of life of this infant that provided the preterm intestinal samples was 60 days. The gestational age of the term infant was 38 weeks. Day of life of the term infant that provided the intestinal samples was 7 days. Human intestinal epithelial stem cells (hIESCs) were isolated from crypts of resected intestine from preterm and term neonates as described previously.[17,18] In brief, 250 crypts are suspended in 25 µL Matrigel as described in Sato's 3-D Matrigel culture system developed for murine intestines.[19] The 25 µL of crypt cell/Matrigel suspension is placed in a 48-well plate. 250 µL/well of enteroid culture medium was then added. The transwell culturing method was adopted from In et al.[20] In brief, 24-well Transwell inserts (Corning 3414) were coated with collagen IV (30 µg/mL). The inserts with collagen IV solution are then incubated at 37 °C for 2 h to ensure successful coating. Cell pellets were resuspended with enteroid culture media supplemented with Y-27632 and CHIR-99021, and seeded onto the apical side of the collagen IV coated Transwell inserts at a density of 750 k/cm^2. Monolayers were then cultured in enteroid culture media for 5 days with media changes every 2 d. On day 5, the culture media was switched to differentiation media for 4 days to induce cellular differentiation. The differentiation media was enteroid culture media in the absence of Wnt3a, r-spondin, Nicotinamide, and SB-202190.[18] A monolayer of hIESCs or differentiated cells on cell culture insert (see Fig. 3a) was then incubated with 10 mM of butyrate for 48 h, followed by released lactate dehydrogenase (LDH) assay for evaluation of cell death.

Human intestinal epithelial cell line (HIEC-6) were isolated by thermolysin treatment from human fetal small intestine at 17 to 19 week gestation, thus largely representing potentially immature intestinal cells. HIEC-6 and human colorectal adenocarcinoma cell line (HT29) were acquired from the American Type Culture Collection (ATCC, Manassas, VA). HIEC-6 cells were cultured in Opti-MEM medium (Gibco) with 4% fetal bovine serum (FBS; Gibco),10 ng/ml EGF (Gibco) and penicillin–streptomycin. HT29 cells were cultured in McCoy's 5A Medium (ATCC) with 10% FBS and penicillin–streptomycin. All cells were cultured in an incubator maintained with 5% CO_2 at 37 °C. HIEC-6 and HT29 cells were incubated with butyrate at indicated concentrations for 48 and 24 h, respectively. 2 µM NSA or 100 µM Nec-1 was used to determine its inhibitory effect on necroptosis with a specific marker pMLKL. Meanwhile, 20 µM of z-VAD (Santa Cruz Biotechnology Inc, Dallas, TX) was used for inhibition of apoptosis, which is detectable using apoptosis-specific markers either cleaved caspase-3 or cleaved K18 antibody.

LDH release assay

Human cultured cells (1×10^5/well) were treated either with or without sodium butyrate in a 24-well plate. After 48 h of incubation at 37 °C in 5% CO_2/air, 100 µL of the supernatant was transferred in triplicate to a 96-well tissue culture plate before adding 100 µL of the Cytotoxicity Detection Kit LDH solution (Takara, Japan) to each well. After 15 min of incubation at room temperature in the dark, its optical density (OD) value was measured at 492 nm in the SpectraMax® i3x multi-mode microplate reader (Molecular Devices, LLC. CA) (620 nm as reference) to detect the total cell death that is non-specific to apoptosis or necroptosis.

Immunohistochemical (IHC) staining

Intestinal samples of neonates with surgical NEC were collected for IHC staining. Specimens were cut into 4–5 µm sections. In brief, tissue sections were deparaffinized in three changes of xylene, and rehydrated three times in an ethanol gradient. Endogenous streptavidin activity was blocked by 0.3% hydrogen peroxide. After antigen retrieval by microwave heating, sections were blocked with 10% serum for 10 min. The slides were incubated with a rabbit anti-p-MLKL antibody (CST, 1:50) for 1 h at room temperature. After washing with PBS, slides were incubated with biotinylated goat anti-rabbit secondary antibody for 30 min at room temperature, and then with horseradish peroxidase–streptavidin for another 30 min. p-MLKL expression was visualized with 3,3'-diaminobenzidine. The sections were counterstained with hematoxylin and mounted in glycergel mounting medium.

Western blot analysis

Whole protein lysates from stool or cells in both rodent and human specimens were prepared using RIPA lysis buffer (Thermo Fisher Scientific,

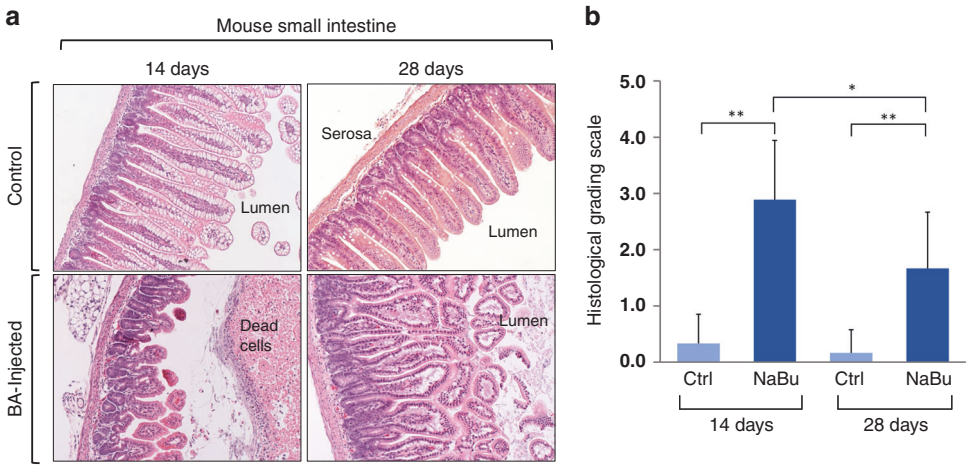

Fig. 1 Intestinal epithelial injury patterns in 14 vs. 28-day mice after intraluminal NaBu-injection. a H&E staining of the mouse small intestinal tissue. **b** Histological grading scale of mouse intestinal epithelium. Note that the younger mice are more susceptable to butyrate-induced cell death in the intestines. NaBu sodium butyrate, Ctrl control. $n = 5$ in each group. The experiment was repeated three times. $^{*}p < 0.05$, $^{**}p < 0.01$.

Rockford, IL). Samples were loaded onto 10% sodium dodecyl sulfate–polyacrylamide gel electrophoresis (SDS-PAGE) gels (BIO-RAD, Hercules, CA), transferred to polyvinylidene difluoride membranes (Amersham Biosciences, Buckinghamshire, UK) and incubated with primary anti-K8 (Troma-1, MilliporeSigma, 1:500), anti-PGC-1α (Abcam, Cambridge, MA, 1:500), anti-phospho-MLKL (p-MLKL) (CST, 1:500), anti-AKT (CST, 1:500), anti-cleaved caspase 3 (CST, 1:500), anti-GAPDH (CST, 1:1000), anti-cleaved-K18 (AnaSpec,Inc., Fremont, CA, 1:1000), anti-4-HNE (Sigma-Aldrich, 1:1000), and anti-β-actin (abcam, 1:2000) antibodies overnight at 4 °C. Membranes were incubated with secondary monoclonal goat anti-rat antibodies (Immunoreagents, Inc., Raleigh, NC, 1:2000) or goat anti-rabbit antibody (CST, 1:2000) at room temperature for 1 h. Protein bands were visualized using an ECL detection kit (Thermo Fisher Scientific, Rockford, IL) according to the manufacturer's protocol.

Statistical analysis

Data are presented as means ± SD. The statistical analysis was performed using Student's *t* test (SPSS Statistics, version 19.0, Chicago). $p < 0.05$ was considered statistically significant. The data graphs were made with the GraphPad Prism 5.0 software (Graph-Pad Software, CA).

RESULTS

Luminal butyrate causes NEC-like intestinal epithelial injury in a development-dependent manner in neonatal mice

Prior publications have described the developmental stage-dependent changes in mouse gut morphology and function upon a comparison of 14- and 28-day testing.[21,22] Accordingly, we compared the degree of intestinal injury conferred by butyrate upon intraluminal (terminal ileum) injection in P14 and P28 mice. Sodium butyrate specifically resulted in significant intestinal injury in pre-weaned neonate mice (14-day) compared to post-weaned juvenile mice (28-day) (Fig. 1). Figure 1a demonstrates a significant increase in the number of sloughed dead cells in the lumen with associated hemorrhage, villus structure disruption, and overall thinned mucosal layer following butyrate administration, with the most profound effect observed in the P14 mice. As shown in Fig. 1b, the histological grading scores were significantly higher in butyrate treatment groups of both P14 and P28 mice (2.89 ± 1.05 vs. 0.33 ± 0.52, $p = 0.00004$; 1.67 ± 1.00 vs. 0.17 ± 0.41, $p = 0.002$). However, the scores in P14 mice significantly exceeded those in P28 mice (2.89 ± 1.05 vs. 1.67 ± 1.00, $p = 0.023$).

In addition, to quantify the degree of intestinal epithelial slough and overall injury due to enterocyte death, mouse stool was collected for further evaluation. Increased levels of total fecal protein were observed by Coomassie brilliant blue (CCB) staining in the butyrate-treated 14-day test group (Fig. 2a, upper panel). Collectively, these proteins are derived from enterocytes and non-enterocyte sources including circulating inflammatory and resident immune cells. K8 is a major component of the intermediate filaments of single-layered epithelia, K8 can therefore be utilized as a quantitative biomarker of intestinal injury and epithelial cell specific loss as previously described.[23] IF staining showed abundant K8 localized specifically to the intestinal epithelial cells but not in other portions of intestinal tissue, blood, or inflammatory cells (Fig. 2b). Therefore, the fecal K8 level was utilized to determine the degree of intestinal epithelial injury. Western blot demonstrated significant quantities of K8 protein in the feces of pre-weaned P14 mice following the intraluminal butyrate injection that was distinct from P28 mice (Fig. 2a, lower panel). These findings demonstrate a developmental stage-dependent feature as pre-weaned P14 mice are far more susceptible to butyrate-induced intestinal injury than juvenile mice (P28).

Butyrate induces more cell death in human intestinal organoid cells of preterm infants through necroptosis

Both human intestinal stem and differentiated cells of preterm and term infants (10^5/well) were seeded in the insert of a 12-well plate (Fig. 3a). The cells were treated with 10 mM sodium butyrate for 48 h, and then the supernatants were collected for LDH assay. The total cell lysates were collected for Western Blot. After 48 h, there was significantly more cell death in differentiated cells of the preterm group compared with the term group (OD value, 0.33 ± 0.12 vs. 0.11 ± 0.03, $p = 0.038$). Similarly, there was a trend toward increased death in stem cells of the preterm group, although the difference was not statistically significant (OD value, 0.20 ± 0.03 vs. 0.08 ± 0.07, $p = 0.068$) (Fig. 3b).

To identify the mechanism of butyrate-induced cell death in human intestinal organoid cells, we determined protein expression levels of the key components in the apoptotic and necroptotic signaling pathways as well as survival-associated proteins using western blot. The results showed that the expression of p-MLKL, a marker of necroptosis, was significantly more upregulated in the preterm group after being treated with butyrate (0.64 ± 0.08 vs. 0.39 ± 0.06, $p = 0.011$). Of note, cleaved caspase-3, a marker of apoptosis, was significantly more upregulated in the term group (1.01 ± 0.19 vs. 0.69 ± 0.14, $p = 0.036$). PGC-1α and AKT (main regulators of mitochondrial biogenesis and cell survival) were downregulated after butyrate treatment in both the term and preterm groups (Fig. 3c).

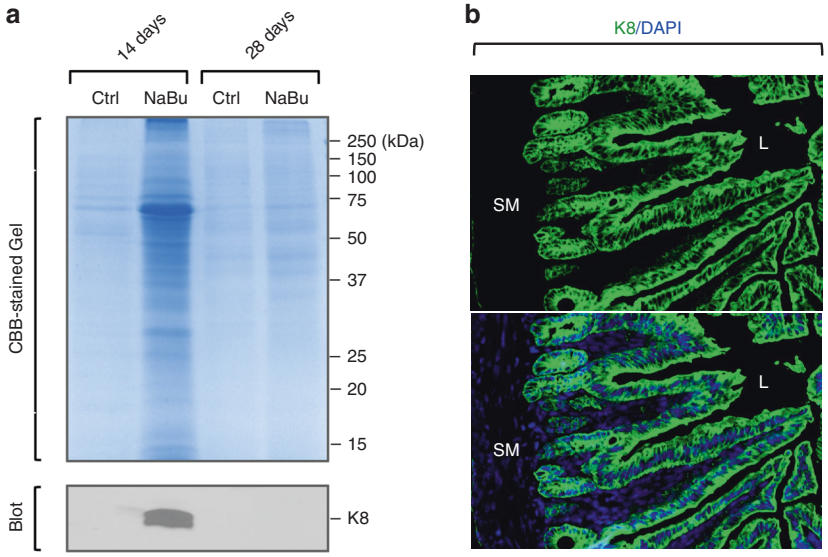

Fig. 2 Fecal K8 was used as a marker of intestinal epithelial injury. a CBB staining and Western Blot results of fecal K8 from 14 or 28-day mice treated with NaBu. K8 keratin 8, CBB coomassie brilliant blue, Ctrl control. **b** Immunofluorescence staining of K8 in mouse intestinal epithelium. L lumen, SM submucosa.

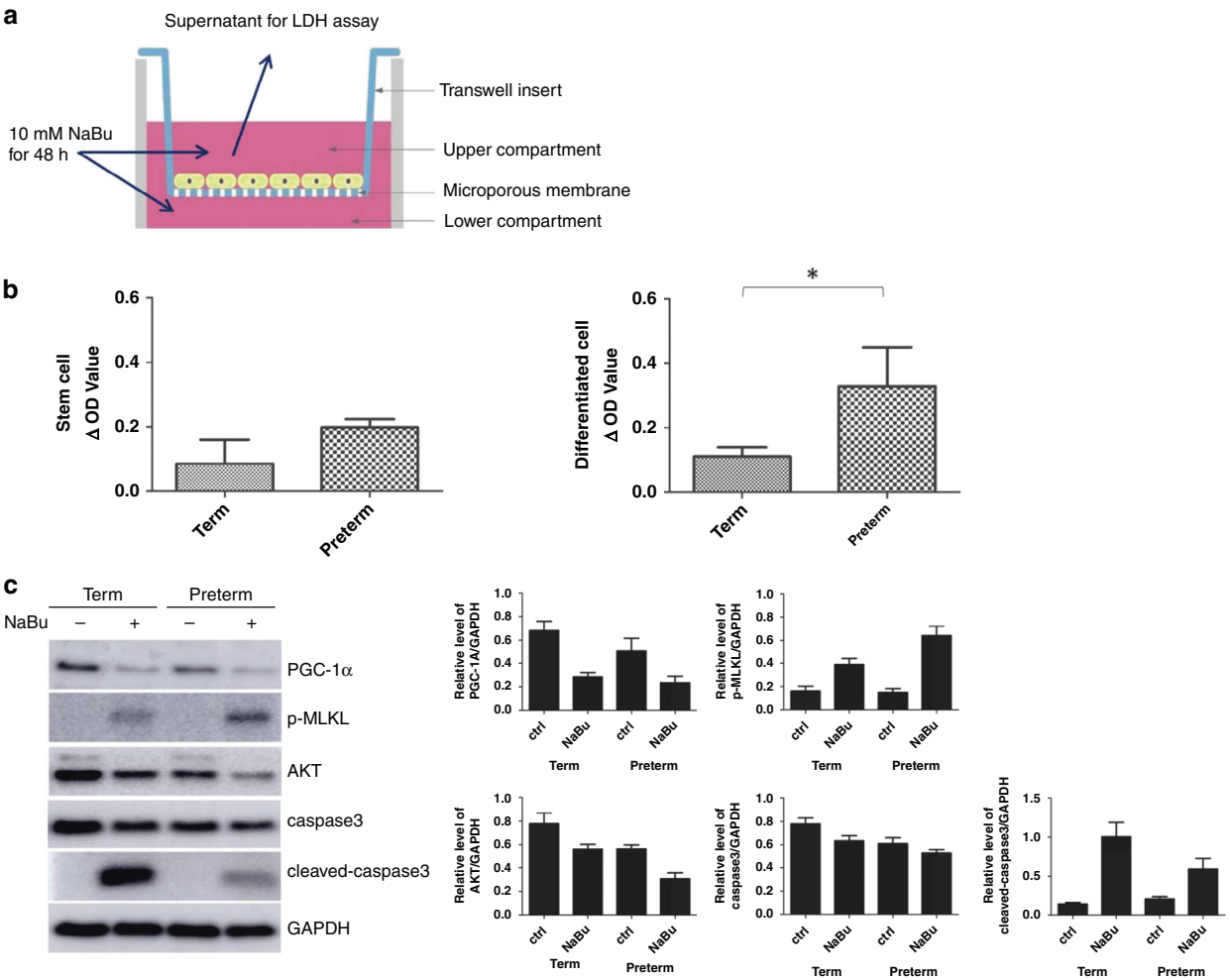

Fig. 3 NaBu induced cell death in human intestinal cells of preterm infants though necroptosis. a Cell culture and NaBu treatment in human intestinal epithelial cells. **b** LDH assay for the detection of cell death induced by NaBu. ΔOD value = OD value of test group − OD value of control group. **c** Western blot results of cell death and survival associated protein. LDH lactate dehydrogenase. The results are representative of three separate experiments. *$p < 0.05$.

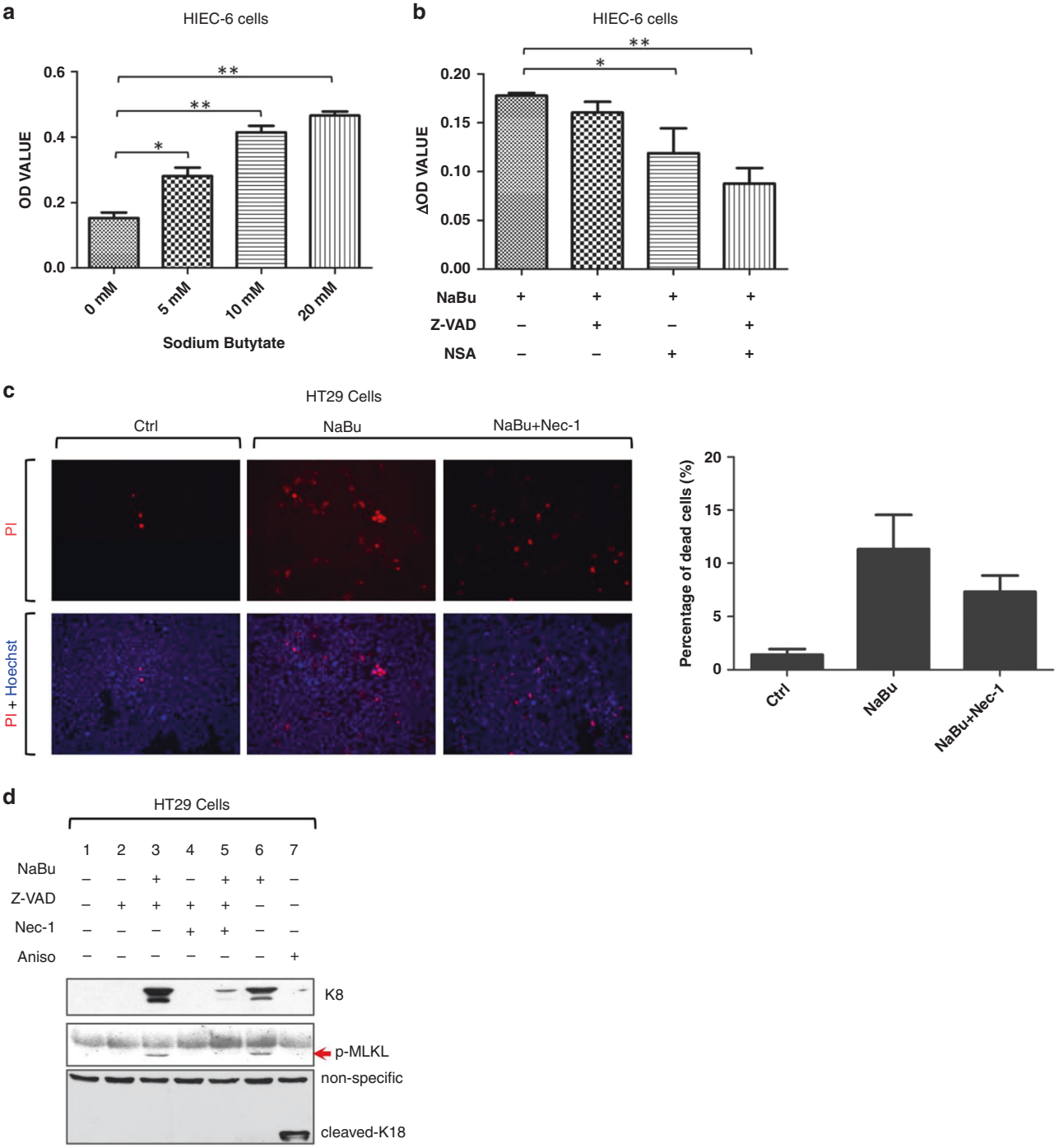

Fig. 4 NaBu induced cell death by necroptosis in HIEC-6 and HT29 cells and the effect of necroptosis inhibitors on cell death. a LDH assay for cell death induced by NaBu at different dose(s) in HIEC-6 cells. **b** NSA inhibits cell death induced by NaBu in HIEC-6 cells. ΔOD value = OD value of test group − OD value of control group. **c** IF staining of PI in HT29 cells treated with NaBu, NaBu/Nec-1, or without NaBu. **d** WB analysis of K8 (for total cell death) and p-MLKL in culture supernatants, and cleaved K18 in attached cells. Z-VAD is an apoptosis inhibitor. NSA or Nec-1 are necroptosis inhibitors. Aniso was used as an apoptosis inducer. Aniso anisomycin, PI propidium iodide. The experiment was repeated three times. *$p < 0.05$, **$p < 0.01$.

Necroptosis inhibitors alleviate intestinal epithelial injury induced by butyrate both in vitro and in vivo

LDH assay results showed that butyrate-induced cell death is dose-dependent in HIEC-6 cells (5–20 mM) (Fig. 4a). 10 mM of sodium butyrate was recognized as the optimal dose to induce cell injury. 2 μM NSA (a necroptosis inhibitor) significantly decreased the cell death induced by butyrate (OD Value, 0.178 ± 0.003 vs. 0.119 ± 0.026, $p = 0.017$), but there was no significant protective effect by 20 μM z-VAD (a pan-caspase inhibitor) alone on butyrate-induced cell death (0.178 ± 0.003 vs. 0.16 ± 0.11, $p = 0.058$) (Fig. 4b).

Moreover, in vitro inhibitory effect of Nec-1 (a necroptosis inhibitor) on butyrate-induced cell death was also confirmed by fluorescence labeling of dead HT29 cells with PI (Fig. 4c). Butyrate-induced cell death (middle column) demonstrated by positive PI-staining (red color) was greatly reduced by the addition of 100 μM Nec-1 to the culture medium (right column). As shown in Fig. 4d,

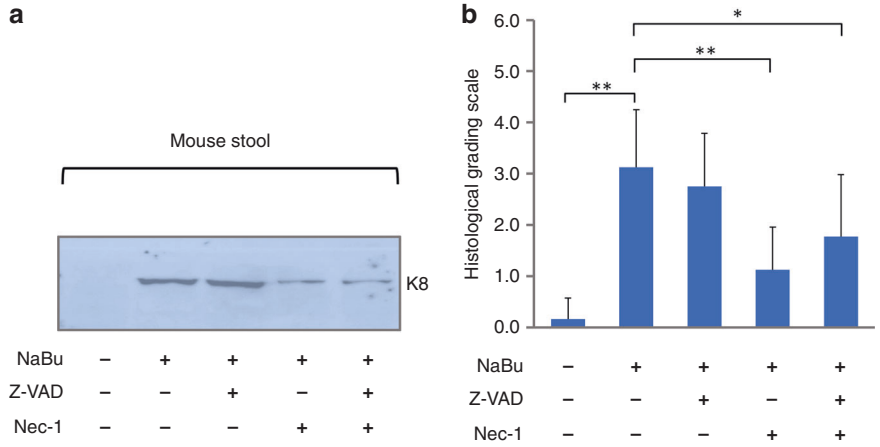

Fig. 5 Necrostatin-1 reduces intestinal epithelial injury in response to intraluminal NaBu-injection in a 14 day mouse model. a Western blot for fecal K8 following intraluminal NaBu-injected mice treated with different reagents. Fecal K8 is used as total cell death marker. **b** Histological grading scale of intestinal epithelia from intraluminal NaBu-injected mice treated with different reagents. $n = 8$ in each group. The results are representative of three separate experiments. *$p < 0.05$, **$p < 0.01$.

cell death (lanes 3, 5, 6, 7) was also detected through the assessment of released K8 in the supernatant. Upon treatment with butyrate, enterocytes died primarily through necroptosis (lanes 3, 5, 6) evidenced by increased p-MLKL but not apoptosis evidenced by lack of the cleaved-K18 which is normally induced by Caspases during apoptosis. Anisomycin was used as an apoptosis inducer for the positive control (lanes 7). The effect of Nec-1 on preventing butyrate-induced injury and cell death was most pronounced when it was used as a single agent. Notably, necroptosis was significantly inhibited by Nec-1 (lane 3 vs. 5) as assessed by p-MLKL.

To further evaluate the in vivo protective effect of Nec-1 on intestinal epithelial injury induced by butyrate, pre-weaned (P14) mouse intestinal lumens were injected with 150 mM sodium butyrate, with and without 200 μM Nec-1 or 40 μM z-VAD, and harvested after 24 h. PBS (1×) was used as a treatment control. Mouse stool samples were collected for detection of fecal K8 through Western Blot. Fecal K8 level was reduced by Nec-1, but not by apoptosis inhibitor z-VAD compared to the NaBu-only group (Fig. 5a). H&E staining and histological grading scale of intestinal epithelia were also conducted to identify the injury. The extent of the injury was significantly weaker in the butyrate + Nec-1 group than in the butyrate-only group (scale, 1.125 ± 0.835 vs. 3.125 ± 1.126, $p = 0.001$) (Fig. 5b).

Necroptosis is involved in the pathogenesis of human NEC

To determine whether necroptosis is involved in human NEC, intestinal specimens from patients with NEC undergoing surgery during the acute episode were examined. IHC staining of resected intestine demonstrated intensive staining of p-MLKL in the intestinal crypts (Fig. 6a, b). p-MLKL-positive enterocyte staining specifically located at the apical membrane of enterocytes (arrows in Fig. 6c, d). Importantly, p-MLKL staining was only observed in NEC affected intestine but not in control samples (Fig. 6e). In addition, rabbit isotype IgG was used as a negative control, but it did not stain the apical membranes of the enterocytes as did the p-MLKL antibody (Fig. 6f).

NaBu induces more oxidative stress in a 14-day-old mouse model

Intestine tissues were collected from two age groups of mice 24 h after luminal injection of 1× PBS control or NaBu. There is a lower level of 4-HNE in the intestinal tissues of P14 mice under physiological conditions compared to P28 mice; however, it was significantly elevated in P14 mice upon NaBu treatment (Supplementary Fig. 1a). The level of lipid peroxidation products (4-HNE) detected in intestinal tissue of P14 mice increased 10.2-fold after NaBu treatment but only increased 1.3-fold in P28 mice (Supplementary Fig. 1b).

DISCUSSION

NEC is among the leading causes of death and disability of preterm and VLBW neonates.[24,25] Premature infants are at increased risk for NEC resulting from biological features including intestinal dysbiosis and metabolic dysfunction.[26,27] Intestinal immaturity as a contributing feature of NEC is well documented and characterized by abnormal absorptive capacity, poor gastrointestinal motility, and an altered gut microbiome.[2–5] These physiologic differences may lead to intestinal stasis of enteric food substances yielding an increased opportunity for bacterial fermentation of undigested carbohydrates and the accumulation of luminal SCFAs. Although modest amounts of SCFAs are essential for normal intestinal health, elevated levels of SCFAs, specifically butyrate may have deleterious effects on mucosal integrity depending on the state of differentiation of the exposed cell types.[7,28] Butyrate has an anti-inflammatory effect and at low concentration maintains intestinal barrier function.[29,30] At physiologic concentrations, butyrate may inhibit intestinal stem cell and progenitor cell proliferation. Differentiated enterocytes of the mature intestine can metabolize a range of butyrate concentrations thereby buffering luminal content and preventing it from reaching stem/progenitor cells exposure and potential toxicity within the crypts.[12,31] The underdeveloped intestine of premature infants has shorter crypts and more superficial stem cells perhaps adding to the intestinal epithelial metabolic vulnerability to butyrate injury.

Rodent intestines in the second week of life (14 days) morphologically and physiologically approximate human intestines in the early third trimester. Many scholars have reported that proinflammatory responses peak at 2 weeks in the murine gut at a time when epithelial barrier function remains immature.[32,33] In the current study, we compared butyrate-induced gut injury in P14 and P28 mice demonstrating more severe injuries in P14 mice after intraluminal butyrate injection. These results revealed that luminal butyrate causes NEC-like intestinal epithelial injury in a development-dependent manner. Moreover, butyrate toxicity appeared to induce cell death in both undifferentiated and differentiated hIESCs, and the effect was more obvious in cells derived from preterm infants.

Necroptosis, a form of regulated necrosis, is one of the main mechanisms of cell death under pathological conditions such as ischemic injury and oxidative stress.[34,35] Like apoptosis, necroptosis can be induced by TNFα and other death receptor ligands.

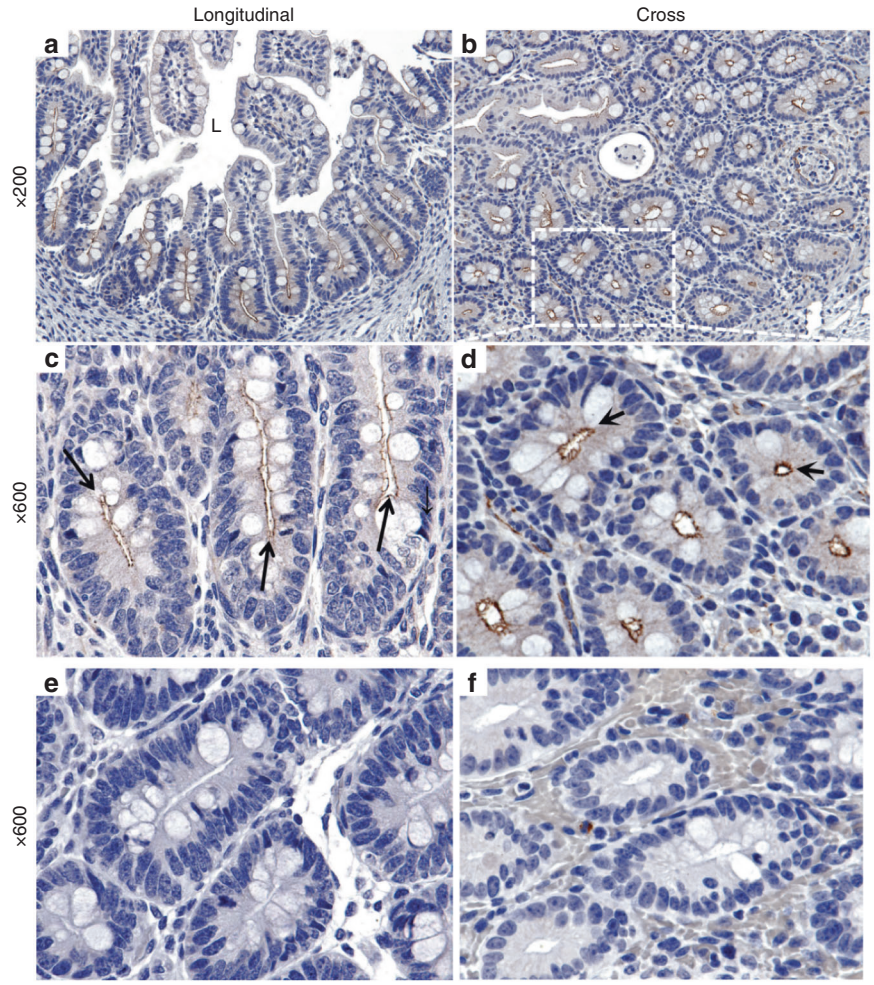

Fig. 6 Necroptotic signaling is activated in the intestinal epithelia of patients with NEC. a, **b** IHC staining of p-MLKL in NEC intestinal epithelia (×200). **c**, **d** IHC staining of p-MLKL in NEC intestinal epithelia (×600). **e** IHC staining of p-MLKL in control group (×600). **f** Rabbit isotype IgG was used as a negative control (×600). L lumen. Arrows depict the positive staining.

But unlike apoptosis, necroptosis requires the activity of receptor-interacting protein kinase 1 (RIP1) and its' associated kinase, RIP3.[36] Once RIP3 is activated, this triggers the mobilization of MLKL to the cell membrane resulting in increased membrane permeability and cell death through necroptosis.[35,37] The balance between death and survival of intestinal epithelial cells is essential to maintain the integrity of the intestinal barrier and intestinal homeostasis, two key physiologic features that have been noted to be compromised in NEC models and consistent with clinical observations in human NEC. Excessive death of intestinal epithelial cells damages the function of the intestinal barrier, leading to a weakened resistance to pathogenic bacteria. Necroptosis has been associated with intestinal inflammation as seen in inflammatory bowel disease[34,38] and more recently in NEC.[39]

In this study, we demonstrated that p-MLKL is upregulated in intestinal epithelial cells of NEC patients providing evidence for the relevance of necroptosis in the pathogenesis of human NEC. Accordingly, we explored the role of necroptosis in our pre-clinical models of development-dependent butyrate-induced cell death. The key effector molecule of necroptosis, expression of p-MLKL was significantly upregulated in the affected P14 mouse group following exposure to butyrate. The effects of necroptosis inhibitors in the prevention and/or treatment of NEC also has been recently studied.[40,41] We explored the role of NSA and Nec1 in the current study. NSA is a small molecule that binds to MLKL and prevents plasma membrane rupture induced by MLKL.[42] Of note, NSA targets the Cys86 residue of human MLKL and not the mouse MLKL.[43] Nec-1 was used to explore the protective effect of necroptosis inhibitors on butyrate-induced cell death in both in vitro human HT29 cells as well as in vivo premature mouse models. We found that NSA inhibits butyrate-induced cell death in HIEC-6 cells and Nec-1 inhibits the intestinal epithelial cell injury induced by butyrate in both HT29 cells and pre-weaned mice. Consistently and intriguingly, we provide evidence for necroptosis to be the primary form of cell death in the cellular and in vivo models presented herein in response to development-dependent butyrate injury.

There are several unanswered questions that arise from this work. Although increased oxidative stress (see Supplementary Fig. 1) could be one of the causes for triggering necroptosis in the younger mice, the mechanism by which butyrate-induced intestinal epithelial cell injury in preterm neonates occurs predominantly through necroptosis while in term neonates it was mostly through apoptosis is not clear and may relate to the developmental maturity of the intestine as well as its processing and mode of responding to injury signals and damaged cells. Whether the results could be reproduced in other models of NEC still need to be further investigated. More studies are required to determine the practical and effective regimens of necroptosis inhibitors for the treatment and/or prevention of NEC. MLKL, RIP3, and other biomolecules involved in the necroptosis pathway may be viable research targets to identify the pathophysiology of NEC and to introduce new treatment options.

CONCLUSION

In this study, we have observed that enteric luminal butyrate causes developmental stage-dependent intestinal epithelial injury that resembles NEC primarily through the mechanism of cellular necroptosis that can be ameliorated by necroptosis inhibitors. We validate the involvement of necroptosis in human NEC by characterizing the effector molecule p-MLKL through immunostaining localization in intestinal crypts of premature newborns. Necroptosis inhibitors proved effective at significantly ameliorating the enteral toxicity of butyrate and thereby suggest a novel mechanism and approach to the prevention and treatment of NEC in premature newborns.

DATA AVAILABILITY

The datasets generated during and/or analyzed during the current study are available from the corresponding author on reasonable request.

REFERENCES

1. Nathan, A. T. et al. A quality improvement initiative to reduce necrotizing enterocolitis across hospital systems. *J. Perinatol.* **38**, 742–750 (2018).
2. Elgin, T. G., Kern, S. L. & McElroy, S. J. Development of the neonatal intestinal microbiome and its association with necrotizing enterocolitis. *Clin. Ther.* **38**, 706–715 (2016).
3. Eaton, S., Rees, C. M. & Hall, N. J. Current research on the epidemiology, pathogenesis, and management of necrotizing enterocolitis. *Neonatology* **111**, 423–430 (2017).
4. Denning, T. L. et al. Pathogenesis of NEC: role of the innate and adaptive immune response. *Semin. Perinatol.* **41**, 15–28 (2017).
5. Neu, J. & Pammi, M. Pathogenesis of NEC: impact of an altered intestinal microbiome. *Semin. Perinatol.* **41**, 29–35 (2017).
6. Warner, B. B. et al. Gut bacteria dysbiosis and necrotising enterocolitis in very low birthweight infants: a prospective case-control study. *Lancet* **387**, 1928–1936 (2016).
7. Lin, J. et al. Short-chain fatty acid induces intestinal mucosal injury in newborn rats and down-regulates intestinal trefoil factor gene expression in vivo and in vitro. *J. Pediatr. Gastroenterol. Nutr.* **41**, 607–611 (2005).
8. den Besten, G. et al. The role of short-chain fatty acids in the interplay between diet, gut microbiota, and host energy metabolism. *J. Lipid Res.* **54**, 2325–2340 (2013).
9. Jiang, P. et al. Premature delivery reduces intestinal cytoskeleton, metabolism, and stress response proteins in newborn formula-fed pigs. *J. Pediatr. Gastroenterol. Nutr.* **56**, 615–622 (2013).
10. Sylvester, K. G. et al. Acylcarnitine profiles reflect metabolic vulnerability for necrotizing enterocolitis in newborns born premature. *J. Pediatr.* **181**, 80–85.e1 (2017).
11. Szylit, O. et al. Fecal short-chain fatty acids predict digestive disorders in premature infants. *Jpen. J. Parenter. Enter. Nutr.* **22**, 136–141 (1998).
12. Kaiko, G. E. et al. The colonic crypt protects stem cells from microbiota-derived metabolites. *Cell* **165**, 1708–1720 (2016).
13. Thymann, T. et al. Carbohydrate maldigestion induces necrotizing enterocolitis in preterm pigs. *Am. J. Physiol. Gastrointest. Liver Physiol.* **297**, G1115–G1125 (2009).
14. Nafday, S. M. et al. Short-chain fatty acids induce colonic mucosal injury in rats with various postnatal ages. *Pediatr. Res.* **57**, 201–204 (2005).
15. Garg, P. M. et al. Necrotizing enterocolitis in a mouse model leads to widespread renal inflammation, acute kidney injury, and disruption of renal tight junction proteins. *Pediatr. Res.* **78**, 527–532 (2015).
16. McElroy, S. J. et al. The ErbB4 ligand neuregulin-4 protects against experimental necrotizing enterocolitis. *Am. J. Pathol.* **184**, 2768–2778 (2014).
17. Sato, T. et al. Long-term expansion of epithelial organoids from human colon, adenoma, adenocarcinoma, and Barrett's epithelium. *Gastroenterology* **141**, 1762–1772 (2011).
18. VanDussen, K. L. et al. Development of an enhanced human gastrointestinal epithelial culture system to facilitate patient-based assays. *Gut* **64**, 911–920 (2015).
19. Sato, T. & Clevers, H. Primary mouse small intestinal epithelial cell cultures. *Methods Mol. Biol.* **945**, 319–328 (2013).
20. In, J. et al. Enterohemorrhagic *Escherichia coli* reduce mucus and intermicrovillar bridges in human stem cell-derived colonoids. *Cell Mol. Gastroenterol. Hepatol.* **2**, 48–62.e3 (2016).
21. Lu, P. et al. Animal models of gastrointestinal and liver diseases. Animal models of necrotizing enterocolitis: pathophysiology, translational relevance, and challenges. *Am. J. Physiol. Gastrointest. Liver Physiol.* **306**, G917–G928 (2014).
22. Xing, T., Camacho Salazar, R. & Chen, Y. H. Animal models for studying epithelial barriers in neonatal necrotizing enterocolitis, inflammatory bowel disease and colorectal cancer. *Tissue Barriers* **5**, e1356901 (2017).
23. Polari, L. et al. Keratin intermediate filaments in the colon: guardians of epithelial homeostasis. *Int. J. Biochem. Cell Biol.* **129**, 105878 (2020).
24. Fitzgibbons, S. C. et al. Mortality of necrotizing enterocolitis expressed by birth weight categories. *J. Pediatr. Surg.* **44**, 1072–1075 (2009). discussion 1075-1076.
25. Patel, R. M. et al. Causes and timing of death in extremely premature infants from 2000 through 2011. *N. Engl. J. Med.* **372**, 331–340 (2015).
26. Mericq, V. et al. Long-term metabolic risk among children born premature or small for gestational age. *Nat. Rev. Endocrinol.* **13**, 50–62 (2017).
27. Kim, M. et al. Immature oxidative stress management as a unifying principle in the pathogenesis of necrotizing enterocolitis: insights from an agent-based model. *Surg. Infect.* **13**, 18–32 (2012).
28. Pourcyrous, M. et al. Fecal short-chain fatty acids of very-low-birth-weight preterm infants fed expressed breast milk or formula. *J. Pediatr. Gastroenterol. Nutr.* **59**, 725–731 (2014).
29. Hung, T. V. & Suzuki, T. Short-chain fatty acids suppress inflammatory reactions in Caco-2 cells and mouse colons. *J. Agric. Food Chem.* **66**, 108–117 (2018).
30. Chen, G. et al. Sodium butyrate inhibits inflammation and maintains epithelium barrier integrity in a TNBS-induced inflammatory bowel disease mice model. *EBioMedicine* **30**, 317–325 (2018).
31. Qiu, Y. et al. Effect of sodium butyrate on cell proliferation and cell cycle in porcine intestinal epithelial (IPEC-J2) cells. *Vitr. Cell. Dev. Biol. Anim.* **53**, 304–311 (2017).
32. Mirpuri, J. et al. Commensal *Escherichia coli* reduces epithelial apoptosis through IFN-alphaA-mediated induction of guanylate binding protein-1 in human and murine models of developing intestine. *J. Immunol.* **184**, 7186–7195 (2010).
33. Lin, P. W. et al. Lactobacillus rhamnosus blocks inflammatory signaling in vivo via reactive oxygen species generation. *Free Radic. Biol. Med.* **47**, 1205–1211 (2009).
34. Wen, S. et al. Necroptosis is a key mediator of enterocytes loss in intestinal ischaemia/reperfusion injury. *J. Cell. Mol. Med.* **21**, 432–443 (2017).
35. Zhang, T. et al. CaMKII is a RIP3 substrate mediating ischemia- and oxidative stress-induced myocardial necroptosis. *Nat. Med.* **22**, 175–182 (2016).
36. Newton, K. et al. Activity of protein kinase RIPK3 determines whether cells die by necroptosis or apoptosis. *Science* **343**, 1357–1360 (2014).
37. Quarato, G. et al. Sequential engagement of distinct MLKL phosphatidylinositol-binding sites executes necroptosis. *Mol. Cell* **61**, 589–601 (2016).
38. Pierdomenico, M. et al. Necroptosis is active in children with inflammatory bowel disease and contributes to heighten intestinal inflammation. *Am. J. Gastroenterol.* **109**, 279–287 (2014).
39. Werts, A. D. et al. A novel role for necroptosis in the pathogenesis of necrotizing enterocolitis. *Cell Mol. Gastroenterol. Hepatol.* **9**, 403–423 (2020).
40. Li, X. et al. MiR-141-3p ameliorates RIPK1-mediated necroptosis of intestinal epithelial cells in necrotizing enterocolitis. *Aging* **12**, 18073–18083 (2020).
41. Liu, T. et al. Toll-like receptor 4-mediated necroptosis in the development of necrotizing enterocolitis. *Pediatr. Res.* **91**, 73–82 (2022).
42. Dong, W. et al. Protective effect of NSA on intestinal epithelial cells in a necroptosis model. *Oncotarget* **8**, 86726–86735 (2017).
43. Sun, L. et al. Mixed lineage kinase domain-like protein mediates necrosis signaling downstream of RIP3 kinase. *Cell* **148**, 213–227 (2012).

ACKNOWLEDGEMENTS

We are grateful to Dr. Teri A. Longacre for acquisition of IHC images.

AUTHOR CONTRIBUTIONS

K.G.S. and J.D. conceived the study. K.W. and G.-Z.T. contributed to the study design. K.W. drafted the manuscript. K.W., G.-Z.T., P.-Y.L., Z.S., B.L., and M.M. contributed to experiments and data acquisition. K.W., G.-Z.T., P.-Y.L., F.S.-J., T.S., J.D., and K.G.S. contributed to data analysis. F.S.-J. and K.G.S. edited the draft and contributed to the final submitted version. All the authors have read and approved the final manuscript.

COMPETING INTERESTS

The authors declare no competing interests.

ETHICS APPROVAL AND CONSENT TO PARTICIPATE

Caretakers of all the participants had signed written informed consent before participation.

ADDITIONAL INFORMATION

Supplementary information The online version contains supplementary material available at https://doi.org/10.1038/s41390-022-02333-z.

Correspondence and requests for materials should be addressed to Guo-Zhong Tao or Karl G. Sylvester.

Reprints and permission information is available at http://www.nature.com/reprints

Publisher's note Springer Nature remains neutral with regard to jurisdictional claims in published maps and institutional affiliations.